The human transient receptor potential vanilloid 3 channel is sensitized via the ERK pathway

Received for publication, June 8, 2017, and in revised form, October 26, 2017 Published, Papers in Press, October 30, 2017, DOI 10.1074/jbc.M117.801167

Lenka Vyklicka[1], **Stepana Boukalova, Lucie Macikova, Stepan Chvojka, and Viktorie Vlachova**[2]

From the Department of Cellular Neurophysiology, Institute of Physiology Czech Academy of Sciences, 142 20 Prague 4, Czech Republic

Edited by Henrik G. Dohlman

The transient receptor potential vanilloid 3 (TRPV3) channel is a Ca^{2+}-permeable thermosensitive ion channel widely expressed in keratinocytes, where together with epidermal growth factor receptor (EGFR) forms a signaling complex regulating epidermal homeostasis. Proper signaling through this complex is achieved and maintained via several pathways in which TRPV3 activation is absolutely required. Results of recent studies have suggested that low-level constitutive activity of TRPV3 induces EGFR-dependent signaling that, in turn, amplifies TRPV3 via activation of the mitogen-activated protein kinase ERK in a positive feedback loop. Here, we explored the molecular mechanism that increases TRPV3 activity through EGFR activation. We used mutagenesis and whole-cell patch clamp experiments on TRPV3 channels endogenously expressed in an immortalized human keratinocyte cell line (HaCaT) and in transiently transfected HEK293T cells and found that the sensitizing effect of EGFR on TRPV3 is mediated by ERK. We observed that ERK-mediated phosphorylation of TRPV3 alters its responsiveness to repeated chemical stimuli. Among several putative ERK phosphorylation sites, we identified threonine 264 in the N-terminal ankyrin repeat domain as the most critical site for the ERK-dependent modulation of TRPV3 channel activity. Of note, Thr^{264} is in close vicinity to a structurally and functionally important TRPV3 region comprising an atypical finger 3 and oxygen-dependent hydroxylation site. In summary, our findings indicate that Thr^{264} in TRPV3 is a key ERK phosphorylation site mediating EGFR-induced sensitization of the channel to stimulate signaling pathways involved in regulating skin homeostasis.

Transient receptor potential vanilloid 3 (TRPV3)[3] is a thermosensitive ion channel widely expressed in epithelial tissues of the skin, where it plays critical roles in epidermal proliferation, differentiation, hair growth, sensory thermotransduction, itch sensation, and the development of cutaneous pain. A number of stimuli have been shown to activate TRPV3, including warm or noxious temperatures (1–3); endogenous compounds such as farnesyl pyrophosphate or nitric oxide; the naturally occurring aromatic monoterpens carvacrol, menthol, and camphor; and synthetic drugs, of which the most frequently used is 2-aminoethoxydiphenyl borate (2-APB) (see Refs. 4–7 for recent comprehensive reviews). The activity of TRPV3 can be further sensitized by a number of signaling molecules downstream of phospholipase C, including unsaturated fatty acids (8), Ca^{2+}/calmodulin (9, 10), protein kinase C (11), and phosphatidylinositol 4,5-bisphosphate (12). Moreover, among other thermosensitive TRP ion channels, TRPV3 has a unique intrinsic property; it is strongly up-regulated by its own activity (13, 14). This, together with a remarkable gating promiscuity (15), makes the channel extremely sensitive to any type of conformational change and, as a consequence, it is difficult to determine the mechanisms of TRPV3 modulation at the molecular level.

In man, several gain-of-function mutations in TRPV3 that lead to enhanced channel activity have been linked to severe channelopathy, congenital Olmsted syndrome, accompanied by strong skin defects (16, 17). Also, the genetic deletion of the *trpv3* gene in mice leads to an impaired epidermal barrier structure and strong deficits in responses to innocuous and noxious heat (18). A significant breakthrough in our understanding of how aberrant TRPV3 activity relates to skin pathophysiology has been made by Cheng *et al.* (19), who elaborated an observation that the defects in hair morphogenesis in mice deficient in *trpv3* strikingly resemble the mouse phenotype bearing mutations in the epidermal growth factor receptor (EGFR) and its ligand, transforming growth factor-α (TGF-α). Their study demonstrated that in keratinocytes, the TRPV3 channel forms a signaling complex with EGFR, whereby its activity is regulated by EGFR-coupled signaling pathways. A mechanism has been proposed in which a weak constitutive activity of TRPV3 raises the intracellular concentration of calcium, which in turn releases TGF-α that binds to and activates EGFR. A further increase in intracellular calcium downstream of EGFR activation then results in a potentiation of TRPV3. As this potentiating effect could be blocked by inhibitors of phospholipase C (PLC) and mitogen-activated protein kinase ERK, these experiments have indicated that the PLC- and ERK-mediated regulation of TRPV3 could be a primary mechanism required for

This work was supported by Czech Science Foundation Grant 15-15839S and the Grant Agency of Charles University Grant GA UK 74417. The authors declare that they have no conflicts of interest with the contents of this article.

This article contains supplemental Table S1 and Figs. S1–S5.

[1] To whom correspondence may be addressed. E-mail: lenka.vyklicka@fgu.cas.cz.

[2] To whom correspondence may be addressed: Dept. of Cellular Neurophysiology, Institute of Physiology CAS, Videnska 1083, 142 20 Prague 4, Czech Republic. Tel.: 420-241-062-711; Fax: 420-241-062-488; E-mail: viktorie.vlachova@fgu.cas.cz.

[3] The abbreviations used are: TRPV3, transient receptor potential vanilloid subtype 3; EGFR, epidermal growth factor receptor; HaCaT, human keratinocyte cell line; 2-APB, 2-aminoethoxydiphenyl borate; ERK, extracellular signal-regulated protein kinase; AR, ankyrin repeat; ARD, ankyrin repeat domain; PLC, phospholipase-C.

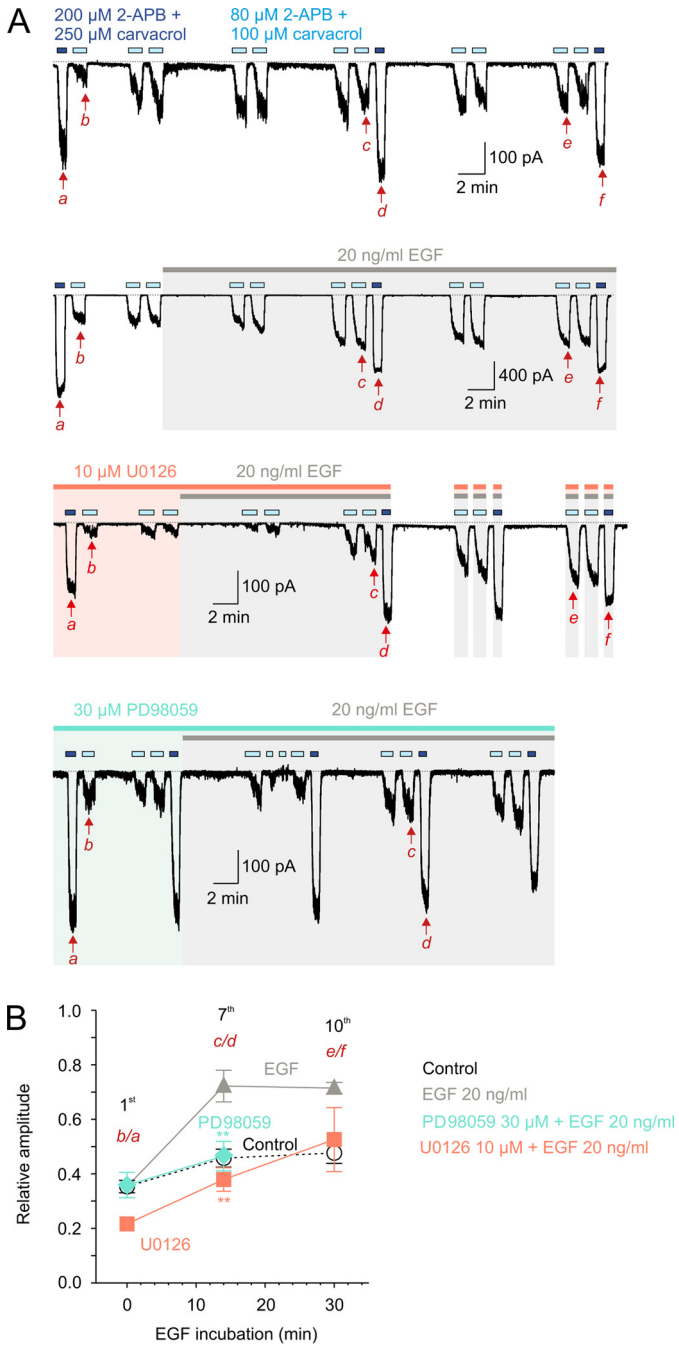

Figure 1. EGF increases potentiation of endogenously occurring TRPV3 channels in HaCaT cells via MAPK signaling pathway. *A,* representative current responses from whole HaCaT cells endogenously expressing TRPV3 channels, repeatedly induced by a mixture of agonists 2-APB with carvacrol at subsaturating (80 with 100 μM, *light blue horizontal bar*) or saturating concentrations (200 μM with 250 μM, *dark blue horizontal bars*) under control conditions and EGF treatment (20 ng/ml, *gray horizontal bar*) either in the absence or presence of MEK inhibitors (10 μM U0126, *orange horizontal bar* and 30 μM PD98059, *cyan horizontal bar*). The baseline is indicated as a *gray interrupted horizontal line*. *Red arrows* and *italic letters* show responses that were used for the statistical analysis in plot *B*. All recordings were measured in the absence of Ca^{2+} ions in extracellular solution at room temperature (23–25 °C) and at −70 mV. For the content of extracellular and intracellular solutions, see "Experimental procedures." *B,* summary plot shows average first, seventh, and tenth current responses evoked by a subsaturating concentration of agonists (corresponding to *b*, *c*, and *e* in *A*) related to the subsequent maximum currents induced by a saturating concentration of agonists (corresponding to *a*, *d*, and *f* in *A*) under control conditions (*white circles*, *dashed line*, $n \geq 5$), after 0, 14, and 30 min incubation with EGF (corresponding to *b*/*a*, *c*/*d*, and e/*f* in *A*) in the absence (*gray triangles*, $n \geq 5$) or presence of MEK inhibitors (U0126: *orange squares*, $n \geq 3$; PD98059: *cyan diamonds*, $n \geq 7$). In cells treated with U0126 or PD98059, the degree of potentiation of the seventh response after the 14-min presence of EGF was only 38 ± 4% ($p = 0.003$, compared with the cells treated with EGF alone; $n = 4$) and 47 ± 5% ($p = 0.008$; $n = 7$), respectively. In the presence of U0126, a prolonged application of EGF (30 min) caused a further sensitization to 53 ± 5%, which was comparable with the relative amplitude obtained in control cells (48 ± 4%; $p = 0.639$; $n = 3$). Data are expressed as mean ± S.E. **, $p < 0.01$.

EGFR-dependent functions (19). Whereas the effects of the PLC-signaling cascade on TRPV3 have been studied intensively at the single-cell level (12, 20), the importance of ERK in mediating TRPV3 potentiation has not been established, and it is unclear whether ERK by itself is sufficient to influence TRPV3.

The activation of EGFR by TGF-α triggers the activation of downstream kinases known as the mitogen-activated protein kinase (MAPK) signaling pathway leading to the final effectors, the extracellular signal-regulated protein kinases 1 and 2 (ERK1/2). These two kinases are generally referred to as ERK because they both exhibit a functional redundancy and no evidence has been provided for a difference in substrate specificity between these two isoforms (21). Although ERK is considered a primary effector of EGFR signaling, it may also integrate other signaling pathways and phosphorylate various ion channels and regulate their gating properties, as is the case with the Cav2.2, Nav1.7, Kv4.2, and TRPC6 channels (22–25).

The sequence analysis of human TRPV3 reveals eight putative phosphoacceptor sites for ERK kinase (S/TP), all present at the cytoplasmic N-terminal end (supplemental Table S1). This part of the protein, as in other members of the vanilloid TRP channel subfamily, features a characteristic ankyrin repeat domain (ARD) consisting of six ankyrin repeats (AR). These ARs are formed by motifs of ~33 amino acid residues that give rise to a structure consisting of two anti-parallel α-helices connected by β-hairpin loops called "fingers." The ARD of TRPV3 has been recently structurally characterized (amino acids Arg^{118}–Ile^{365}) and a functionally important finger from which the TRPV3 channel can be decisively modulated was identified (26). The fact that two of the predicted ERK phosphorylation sites, Thr^{264} and Thr^{343}, are situated within this relatively well defined region raises an interesting possibility that the channel may be modulated by direct phosphorylation at its N terminus. Here we set out to explore whether the activation of EGFR signaling in keratinocytes results in the potentiation of TRPV3 responses through ERK phosphorylation, and to determine the contribution of the predicted phosphorylation sites in this process.

Results

EGF treatment promotes potentiation of TRPV3 currents in keratinocytes via MAPK signaling pathway

We used human keratinocyte HaCaT cells and the whole-cell patch clamp technique to study the effects of EGF on the activity of endogenously expressed TRPV3 channels. To identify TRPV3-expressing cells, a combination of two TRPV3 agonists 2-APB and carvacrol at saturating concentrations (200 and 250 μM) was first briefly applied to a cell (Fig. 1*A*). If a cell displayed a detectable current response at a holding potential of −70 mV (~40% of cells), a combination of subsaturating concentrations of 2-APB and carvacrol (80 and 100 μM) was applied for 30 s and

then repeatedly for two 30-s periods at 5-min intervals. Whereas the responses to the latter combination of agonists subsequently increased, the maximum response to a combination of higher concentrations of agonists remained largely unchanged, and was regularly tested for rundown correction. This protocol enabled us to assess the degree of potentiation induced by EGF that runs in parallel with the use-dependent sensitization that is intrinsic to the TRPV3 channel (14). TRPV3 responses were recorded either under control conditions or in the continuous presence of EGF, applied with or without one of the two different selective mitogen-activated protein kinase (MEK) inhibitors U0126 or PD98059. The first (b), seventh (c), and tenth responses (e) were normalized to a subsequent maximal saturating response (corresponding to b/a, c/d, and e/f in Fig. 1*A*). Under control conditions, the first response to the combination of subsaturating agonists reached 35 ± 2% of the maximum response and was potentiated upon the seventh and tenth application to 46 ± 3 and 48 ± 4% (Fig. 1*B*), respectively. The cells treated with EGF (20 ng/ml, 14 min) exhibited a seventh response that reached 72 ± 6% of the maximum response. Prolonged incubation with EGF (30 min) did not cause any further increase (72 ± 2%). Consistent with previous reports (19), the amplitude of TRPV3 responses induced by saturating concentrations of the agonists was not affected by the presence of EGF.

To determine whether the potentiating effect of EGF is mediated by the MAPK signaling pathway, two different MEK inhibitors, U0126 (10 μM) and PD98059 (30 μM), were tested together with EGF. The treatment of the cells with either of the two inhibitors completely abolished the potentiating effect of EGF on TRPV3 currents (Fig. 1*B*). In cells treated with U0126 or PD98059, the degree of potentiation of the seventh response after the 14-min presence of EGF was only 38 and 47%, respectively. In the presence of U0126, a prolonged application of EGF (30 min) caused a further potentiation to 53 ± 5%, which was comparable with the relative amplitude obtained in control cells. Together, these experiments confirm previous observations obtained in mouse primary keratinocytes (19) and suggest that the potentiating effect of EGF on TRPV3 is mediated via MEK kinases, whose direct substrate ERK1/2 kinase may phosphorylate TRPV3.

Thr^{264} represents a potential ERK phosphorylation site

To examine whether the potentiating effect of EGF on TRPV3 responses in HaCaT cells can be mediated by the phosphorylation of TRPV3, we used several prediction servers to assess potential phosphorylation sites for ERK (supplemental Table S1). In total we identified eight ERK1/2 consensus sites (P*X*(S/T)P) at the N terminus of human TRPV3, four of them containing a P*XSP* motif (Ser^{60}, Ser^{85}, Ser^{88}, and Ser^{102}) and the next four a P*X*TP motif (Thr^{35}, Thr^{96}, Thr^{264}, and Thr^{343}). We individually replaced all these serines and threonines with aspartic acid to mimic the negative charge of the phosphate group. The mutants were transiently transfected to HaCaT cells and assayed electrophysiologically using repeated stimulations with a low concentration of 2-APB (50 μM), applied four times for 30 s with 30-s intervals and followed by a 10-s application of a combination of 2-APB (200 μM) with carvacrol (150 μM) to obtain a reference saturating response (Fig. 2*A*).

In wild-type TRPV3, the inward currents subsequently increased upon repeated stimulation with 2-APB, on the fourth application reaching about 5% of the saturating response (Fig. 2*B*). The T264D mutant produced significantly larger first responses than the wild-type channels. When 2-APB currents were normalized to the reference saturating response for a given cell, two additional mutants, S85D and S102D, were identified to produce significantly larger first responses than the wild-type channels (supplemental Fig. S1). Two of the mutant channels, T264D and T343D, did not exhibit any sensitization upon repeated stimulation with 2-APB. In T264D, the first response reached about 7% of the maximum response, which was not significantly different from the fourth response. In contrast to the currents through wild-type channels, the majority of T264D responses to 2-APB apparently reached a plateau during 30 s of application. The 2-APB currents through T343D were barely detectable, being significantly smaller than those of wild-type channels and the other mutants. The fourth response in T343D remained at the initial level of 0.3% of the maximum, indicating functional rather than phosphorylation-mimicking effects. The T35D construct yielded also a significantly smaller initial response to 2-APB but exhibited sensitization comparable with wild-type channels. Apart from S85D, for all the mutants tested, maximal inward currents elicited by the combination of saturating agonists were not statistically different from wild-type channels.

Taken together, these findings identify threonine 264 as the most likely candidate to be a phosphorylation site for ERK1/2, because the phosphomimicking mutation sensitized the channel without affecting its maximum responses, as would be expected for the potentiating effect of MEK kinases observed in our experiments. Therefore, we set out to further characterize the effects of other substitutions at this key residue to assess its role in TRPV3 channel functionality.

Phosphomimicking/phosphonull mutations at Thr^{264} affect TRPV3 functioning

In further experiments, we used the HEK293T expression system to avoid a possible contribution of endogenous TRPV3 channels that are expressed in HaCaT cells, and to examine whether the effects of mutations at Thr^{264} are independent of the expression system used. We measured currents from the T264D mutant channels (Fig. 3*A*) using an analogous protocol to that described above. Moreover, we examined two additional constructs: the alternative phosphomimetic mutation T264E and the phosphonull mutation T264A. T264D and T264E exhibited an identical phenotype to T264D in keratinocytes, dramatically larger responses to 2-APB that did not sensitize upon repeated applications (50 μM, 30 s with 30-s intervals). In these two constructs, the fourth response to 2-APB was not statistically different from the initial response (Fig. 3*B*), whereas that for wild-type channels increased 3-fold and T264A about 2-fold. In T264D, all four 2-APB responses were significantly larger compared with wild-type TRPV3. There was no significant difference in the maximum currents induced by a combination of saturating agonists (200 μM 2-APB and 150 μM carvacrol, 10 s) between the mutants and the wild-type channels. These results indicate that mutations at threonine 264 affect

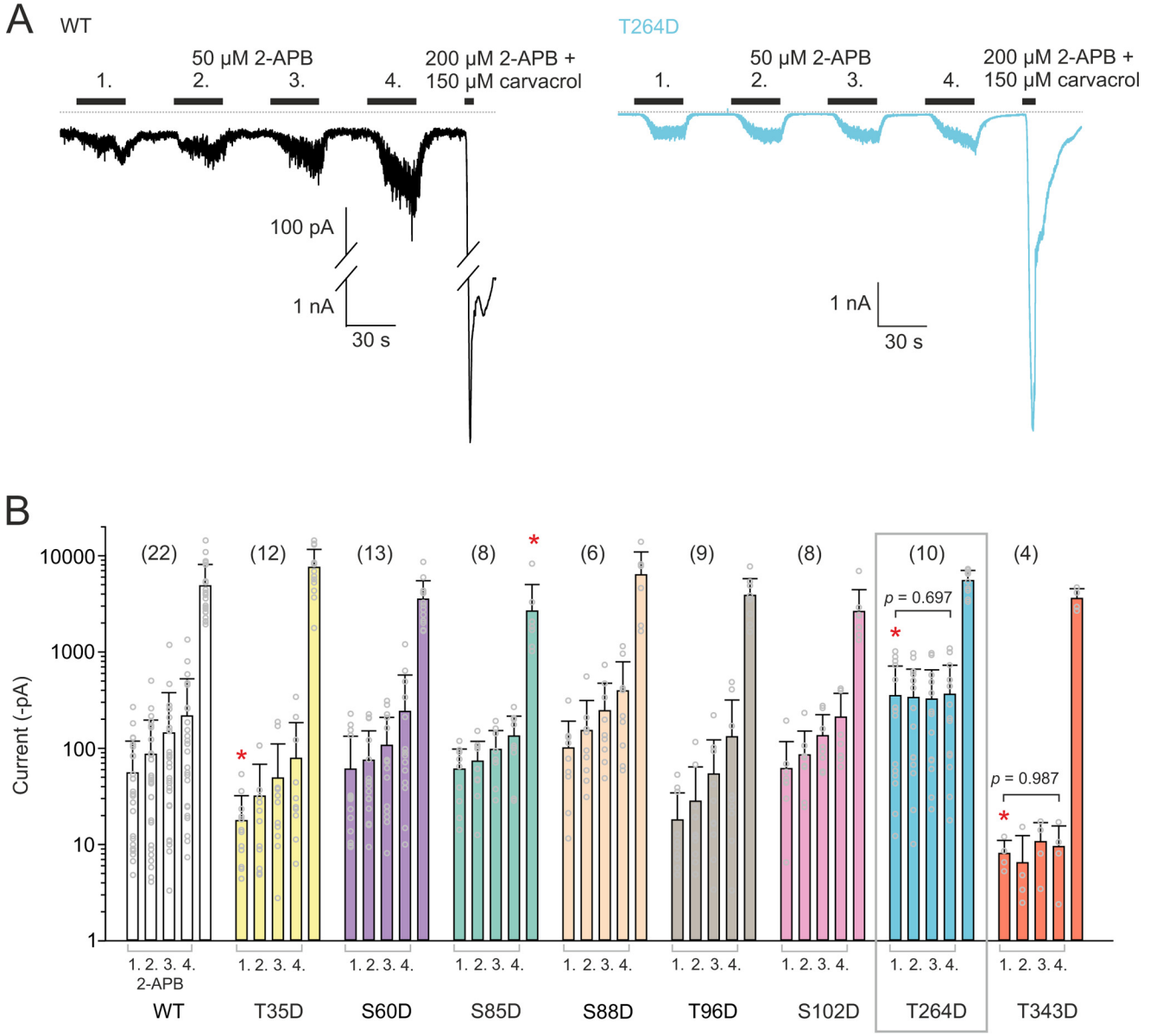

Figure 2. Phosphomimetic mutations of residues at the N terminus of TRPV3 channel revealed Thr^{264} residue as the most likely candidate to be the target of ERK kinase. *A,* representative current responses from whole HaCaT cells transiently transfected with human TRPV3 (*black* recording) and its mutant variant T264D (*blue* recording) induced by repeated applications of 50 μM 2-APB (×4, 30 s) and by a mixture of agonists at their saturating concentrations (200 μM 2-APB and 150 μM carvacrol, 10 s). Wild-type responses to 2-APB were markedly smaller compared with that induced by the mixture of agonists. Therefore two current scales were used. The holding potential was −70 mV. *B,* summary plot of average amplitudes (in logarithmic scale) evoked by four (*1–4*) consecutive 2-APB applications followed by the mixture of agonists corresponds to *panel A* recordings for wild-type (*white* bars) and aspartic acid mutants (*colored bars*). The T35D construct yielded a smaller initial response to 2-APB ($p < 0.041$, see also supplemental Fig. S1) but exhibited potentiation of the fourth response not significantly different from wild-type channels (3.3 ± 0.5-fold; $p = 0.606$). The T264D mutant produced significantly larger first responses than the wild-type channels (one-way analysis of variance with Dunnett's post hoc test, $p < 0.001$). In this mutant, the first response reached 6.7 ± 3.2% of the maximum response, which was not significantly different from the fourth response, which reached 7.1 ± 3.1% of the maximum amplitude ($p = 0.697$; paired *t* test). The 2-APB currents through T343D were barely detectable, being significantly smaller than those of wild-type channels and the other mutants (Student's *t* test, $p = 0.03$). The fourth response in T343D remained at the initial level of 0.3% of the maximum ($p = 0.987$; paired *t* test), indicating functional rather than phosphorylation-mimicking effects. Apart from S85D (2.7 ± 0.8 nA; one-way analysis of variance, $p = 0.007$), for all the mutants tested, maximal inward currents elicited by the combination of saturating agonists were not statistically different from wild-type channels (4.8 ± 0.9 nA). Data are shown as mean ± S.D. *, $p < 0.05$. *n* are indicated in *brackets*. See also supplemental Fig. S1.

TRPV3 functioning in a manner consistent with persistent or lacking phosphorylation.

Overexpression of ERK1 supports the specific role of Thr^{264} in TRPV3 phosphorylation

To further explore whether the ERK kinase may functionally affect TRPV3, ERK1 was transfected to HEK293T cells together with the wild-type TRPV3 channel. The presence of ERK1 in cells caused a strong increase in 2-APB responses (Fig. 4*A*). Upon repeated stimulation, the currents did not exhibit statistically significant sensitization, and their fourth responses reached 11.5 ± 3.3% of the maximum amplitude induced by saturating concentrations of 2-APB and carvacrol. The saturating responses trended toward lower values in the presence of ERK1, although the difference did not reach statistical significance ($p = 0.085$). Next, the cells were cotransfected with ERK1

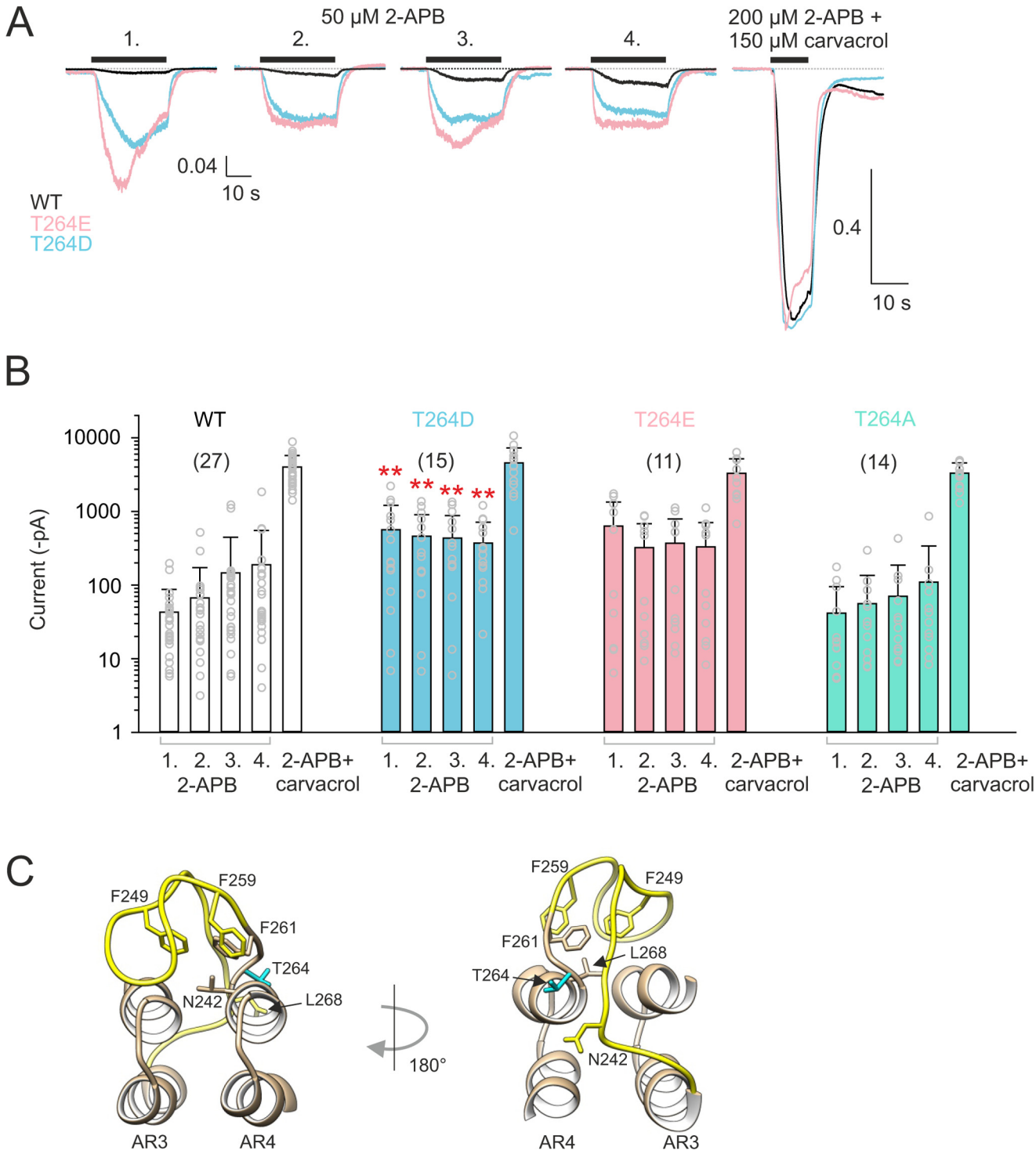

Figure 3. Replacing threonine 264 with negatively charged residues caused pre-sensitized TRPV3 channel in HEK293T cells. *A,* time courses of average responses from analogous experiments as described in the legend to Fig. 2*A*, normalized to the maximum currents evoked by the saturating concentration of agonists (200 μM 2-APB with 150 μM carvacrol). Agonists were applied for the time indicated by the *black horizontal bar*. Baseline was set at 0 level. *B,* average amplitudes (in logarithmic scale) from wild-type (*white bars*), T264D (*blue bars*), T264E (*pink bars*), and T264A (*cyan bars*) mutants induced by four applications of 50 μM 2-APB and then by the combination of 200 μM 2-APB with 150 μM carvacrol corresponding to the protocol as described in the legend to Fig. 2*A*. In T264D and T264E, the fourth response to 2-APB was not statistically different from the initial response ($p = 0.303$ and 0.232, paired *t* test), whereas that for wild-type channels the response increased 3-fold and for T264A the response was about 2-fold. In T264D, all four 2-APB responses were significantly larger compared with wild-type TRPV3. There was no significant difference in the maximum currents induced by the combination of saturating agonists between the mutants and the wild-type channels (one-way analysis of variance, $p = 0.119$). The data represent mean ± S.D., **, $p \leq 0.01$. *n* are indicated in *brackets*. *C,* threonine 264 is predicted to be accessible for phosphorylation. The Thr^{264} residue (*blue*) shown in the context of ankyrin repeats 3 and 4 (*AR3* and *AR4*) of the mouse TRPV3-ARD structure (Protein Data Bank code 4N5Q), finger 3 is shown in *yellow*. The key hydrophobic residues responsible for the bending of finger 3 are depicted (Phe^{249}, Phe^{259}, and Phe^{261}, Leu^{268} from the inner helix of repeat 4). The hydroxylation site Asn^{242} is shown.

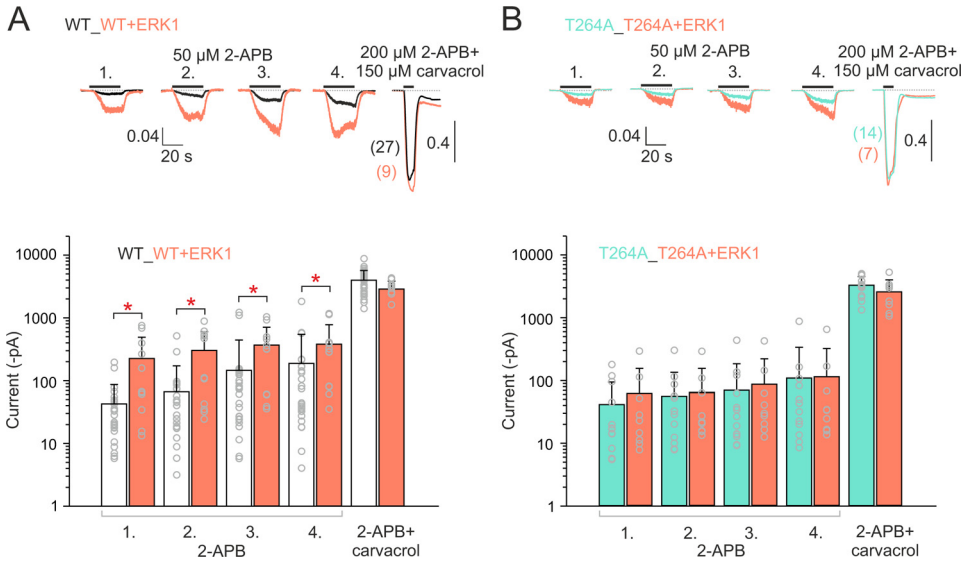

Figure 4. Overexpression of ERK1 kinase increased 2-APB-induced responses of TRPV3 channels in Thr^{264}-dependent manner. *A, upper*: the time course of average currents through transiently transfected wild-type TRPV3 channels in HEK293T cells, normalized to the maximum currents evoked by saturating concentration of agonists, induced by repeated 2-APB stimulations (×4, 30 s, 50 μM) with (*orange*) or without ERK1 (*black*). Agonists were applied for the time indicated by the *black horizontal bar*. *Below*: the bar graph represents absolute amplitudes (in logarithmic scale) from recordings shown above. Overexpression of ERK1 increased all four 2-APB responses ($p = 0.016$, 0.010, 0.016, and 0.024). Upon repeated stimulation, the currents did not exhibit statistically significant sensitization in ERK1 expressing cells ($p > 0.153$; paired *t* test). Colors and *n* are as described above. *B,* identical protocol as in *A* was used for T264A mutant. *Upper*: the time course of normalized currents from the transiently transfected T264A mutant in HEK293T cells induced by repeated 2-APB stimulations with (*orange*) or without ERK1 (*cyan*). 2-APB and carvacrol were applied for the time indicated by the *black horizontal bar*. *Below:* the graph shows the absolute amplitudes of the T264A mutant from the same experiments as above with and without ERK1. The 2-APB currents through T264A coexpressed with ERK1 exhibited amplitudes not significantly different from cells transfected with T264A alone ($p = 0.548$, 0.640, 0.423, and 0.841). Colors and *n* are as shown above. Data are mean ± S.D. *, $p \leq 0.05$.

together with the phosphonull T264A mutant (Fig. 4*B*). The 2-APB currents through T264A coexpressed with ERK1 exhibited amplitudes not significantly different from cells transfected with T264A alone. Likewise with wild-type channels, the maximum response induced by a saturating combination of agonists was slightly, but not significantly smaller ($p = 0.230$). Thus, the wild-type channels in the presence of ERK1 kinase exhibit larger initial responses to 2-APB that do not further sensitize, similar to those in the phosphomimetic mutants T264D and T264E (compare Fig. 4*A* and Fig. 3, *A* and *B*). Taken together, these results support a possible role of Thr^{264} in the ERK1-mediated phosphorylation of the human TRPV3 channel.

T264A mutation results in a substantial decrease in EGF-mediated potentiation

To further confirm the role of Thr^{264} in EGF-induced sensitization, wild-type or T264A were transiently transfected to HaCaT cells and assayed electrophysiologically using repeated stimulations with a low concentration of 2-APB, applied four times for 10 s with 30-s intervals, first in the absence and then in the continuous presence of EGF (20 ng/ml; Fig. 5). EGF was pre-applied for 1 min before the fifth 2-APB application. At the end of the series, a combination of 2-APB (200 μM) with carvacrol (150 μM) was applied for 10 s to obtain a reference saturating response. Compared with the initial 2-APB response, the 8th response increased about 6-fold in WT and 4-fold in T264A. Whereas the fourth response through TRPV3 measured in the presence of EGF reached 11% of the maximum response, the mutant channels exhibited only 2% increase, thus supporting a key role of Thr^{264} in EGF-induced potentiation.

Discussion

In this study, we identify threonine 264 in the N-terminal ARD as a putative site for the ERK1-dependent modulation of TRPV3. This conserved residue is located at the beginning of the inner helix of repeat 4, forming part of the general conserved TPLA consensus sequence of the repeat. Although the overall fold of TRPV3-ARD is shared with other TRPV channels, recent structural analysis revealed an apparent uniqueness of this domain (26). In TRPV3, finger 3 atypically bends over toward finger 2 and is stabilized by interactions with the inner helix of repeat 3 (Fig. 3*C*). The authors of the study demonstrated that mutations disrupting hydrophobic interactions stabilizing the finger 3 conformation severely affect TRPV3 sensitivity to 2-APB stimulation. This characteristic region immediately precedes threonine 264, thus implying a possibility that interactions between this residue and ERK1 may alter the conformation of this important loop and powerfully influence the channel's activation. Besides this, finger 3 contains a motif including asparagine 242, through which the TRPV3 channel can be effectively regulated by oxygen-dependent hydroxylation (27). Although we cannot exclude the possibility that mutations at Thr^{264} themselves disturbed a local structure near the functionally important finger 3, there are several lines of evidence supporting our conclusion that TRPV3 could be a substrate for ERK-phosphorylation with Thr^{264} as one of the possible targets. First, our experiments obtained from HaCaT cells confirm previous studies in mouse primary keratinocytes (19) and suggest that the potentiating effect of EGF on TRPV3 can be inhibited by two different selective MEK inhibitors, U0126 or PD98059, and hence it is likely mediated via MEK

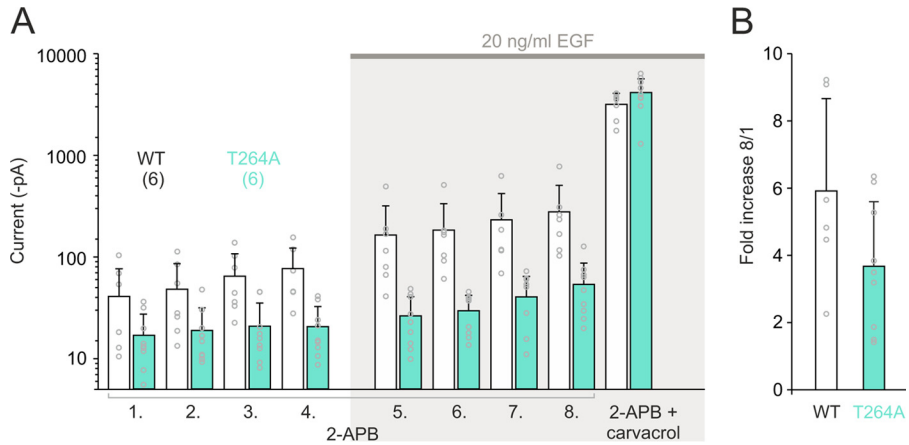

Figure 5. EGF increases inward currents in TRPV3 but less in T264A channels transiently expressed in HaCaT cells. *A,* summary plot of average amplitudes (in logarithmic scale) evoked by four (*1–4*) consecutive 2-APB applications in the absence of EGF, and then by four (*5–8*) consecutive 2-APB applications in the presence of EGF recorded from wild-type (*white bars*) and T264A (*cyan bars*). EGF was pre-applied for 1 min before the fifth 2-APB application. Extracellular and intracellular solutions were used as described in the legend to Fig. 1. The mixture of agonists at saturating concentrations was applied at the end of the series (200 μM 2-APB and 150 μM carvacrol). The eighth response through TRPV3 reached 11.3 ± 14.8% of the maximum response, the T264A mutant channels exhibited only 2.1 ± 3.0% of the saturating response ($p = 0.008$). *B,* the average fold-increase in the 2-APB currents after addition of EGF from experiments as in *panel A* (the eighth response relative to the first response, 8/1; $p = 0.056$). Data are mean ± S.D., *n* are indicated.

kinases. Second, phosphomimetic mutations at Thr^{264} markedly promoted the activity of TRPV3 (Figs. 2 and 3), whereas the unphosphorylatable T264A mutant exhibited slightly ($p = 0.112$) lower fourth responses to the subsaturating agonist (Fig. 3*B*). Third, the overexpression of ERK1 with TRPV3 significantly increased 2-APB responses and prevented their sensitization upon repeated stimulation. This increase was most likely not caused by changes in the level of TRPV3 expression (supplemental Fig. S2). The presence of ERK1, on the other hand, did not affect the nonphosphorylatable T264A mutant. Fourth, T264A mutation resulted in a substantial decrease in EGF-induced potentiation (Fig. 5).

We cannot rule out the presence of some additional phosphorylation site(s) on TRPV3, because a mild increase in 2-APB current responses was observed in cells co-transfected with T264A and ERK1 (Figs. 4*B* and 5). The secondary potential ERK phosphorylation site could be Ser^{102} or less likely Ser^{85} (supplemental Fig. S1). Both of these residues are located at the beginning of the N terminus, outside the ARD, and thus highly accessible to the aqueous environment. Although the phosphomimetic mutations at both these serines increased the first normalized 2-APB response resembling a constitutively phosphorylated channel, the S85D mutation reduced maximal inward currents elicited by the combination of saturating agonists (Fig. 2*B*), which would not be expected from the EGF-mediated effects observed in our experiments (Fig. 1).

Recent mass spectrometric-based large-scale surveys (PhosphoSitePlus database (28)) have identified several *in vivo* phosphorylation sites in human or mouse TRPV3 (Ser^{374}, Thr^{378}, Ser^{387}, Thr^{421}, and Thr^{427}). However, none of these sites fulfills the consensus sequence for ERK. To map putative *in vivo* ERK phosphorylation sites, we subjected TRPV3 purified from HaCaT cells to mass spectrometry (MS) analysis (supplemental Figs. S3–S5). Using TRPV3-transfected HaCaT cells, this approach identified two endogenous phosphorylation sites, Thr^{35} and Thr^{37}, within the peptide sequence RPAEITPTKK. Whereas Thr^{37} does not fulfill the consensus sequence for ERK, the phosphomimetic mutation at Thr^{35} in our experiments shown in Fig. 2*B* led to a significant decrease in initial response to 2-APB but, upon repeated stimulation, the sensitization was comparable with wild-type channels. Therefore, these sites are probably not involved in the observed functional changes. Next, we have purified TRPV3 from HaCaT cells transfected with TRPV3 together with ERK1 in a ratio of 1:1. This situation corresponds to our experiments shown in Fig. 4. The MS analysis did not reveal any clear phosphorylation site, suggesting that the excess ERK1 kinase may change the phosphorylation status of TRPV3. In the sequence comprising Thr^{264} (YQHEGFYFGETPLALAACTNQPEIVQLLMEHEQTDITSR) the phosphorylation has been detected neither in TRPV3-expressing cells nor in TRPV3–ERK1-expressing cells. Clearly more work is needed before the signaling pathways regulating TRPV3 can be fully understood in the context of EGFR-generated signals. In skin tissues and HEK293 cells, EGFR can directly or indirectly associate with TRPV3, and the EGFR activation results in the tyrosine phosphorylation of TRPV3 (19). Thus, other possible phosphorylation sites in addition to Thr^{264} are most likely involved in EGFR-mediated sensitization.

In the study by Cheng *et al.* (19) the authors explored the regulatory mechanisms of TRPV3 activity via the activation of the EGFR receptor in keratinocytes. Based on Ca^{2+} measurements, they suggested that EGFR activation leads to the potentiation of TRPV3 activity, and that this effect is mediated by PLC-dependent and partly by MAPK signaling pathways. In our study, we support these observations by using EGF treatment and inhibitors of MEK activation and the MAPK cascade in a human keratinocyte-derived HaCaT cell line. Moreover, we demonstrate that in the absence of Ca^{2+}, the inhibitors of MEK completely prevent the EGF-induced potentiation of TRPV3 responses (Fig. 1*B*), suggesting that the MAPK signaling pathway may contribute to TRPV3 sensitization independently of the PLC signaling pathway.

In conclusion, the data presented here identify threonine 264 in the N-terminal ankyrin repeat 3 of TRPV3 as a potential

target for ERK-mediated phosphorylation. The close vicinity of this residue from the structurally and functionally important region comprising an atypical finger 3 and oxygen-dependent hydroxylation site adds further complexity to the cellular signaling pathways involved in the regulation of skin homeostasis via growth factor downstream signaling.

Experimental procedures

Cell culture and transfection of HaCaT cells

Human immortalized keratinocytes, HaCaT cells (CLS Cell Lines Service GmbH, Germany), were grown in calcium-free DMEM (GIBCO, Invitrogen) supplemented with 10% fetal bovine solution (FBS) in an atmosphere of 95% air and 5% CO_2 at 37 °C. Cells were split twice a week in a 1:10 ratio using TrypLE express enzyme solution (Thermo Fisher Scientific). In some experiments (Figs. 2 and 5) HaCaT cells were transiently transfected with 150 ng of human TRPV3 (in pcDNA5/FRT vector, kindly provided by Ardem Patapoutian) or its mutated variant, and 300 ng of GFP (Takara, Japan) using Lipofectamine 2000 (Invitrogen). Cells were grown on cover glasses (24 mm diameter) for 24–48 h.

Cell culture and transfection of HEK293T cells

HEK293T cells were cultured in Opti-MEM I medium (Invitrogen) supplemented with 5% FBS as described previously (29). The day before transfection, cells were plated in 24-well plates (2×10^5 cells per well) in 0.5 ml of medium and became confluent on the day of transfection. The cells were transiently co-transfected with 300 ng of cDNA plasmid encoding wild-type or mutant TRPV3 and with 300 ng of GFP plasmid using the magnet-assisted transfection technique (IBA GmbH, Goettingen, Germany) and then plated on poly-L-lysine-coated glass coverslips. In the experiments with ERK1, cDNA plasmid encoding wild-type or mutant TRPV3 was co-expressed with ERK1 (in pEGFP-C1 vector, Addgene, number 14747) and GFP in the cDNA ratio of 300:300:150. At least three independent transfections were used for each experimental group. The wild-type channel was regularly tested in the same batch as the mutants. The cells were used 24–48 h after transfection.

Mutagenesis

The mutants were generated by PCR using a QuikChange II XL site-directed mutagenesis kit (Agilent Technologies) and confirmed by DNA sequencing (GATC Biotech, Germany).

Patch clamp recording

Whole-cell membrane currents were recorded by employing an Axopatch 200B amplifier and pCLAMP 10 software (Molecular Devices, Sunnyvale, CA). Patch electrodes were pulled from a glass tube with a 1.5-mm outer diameter. The tip of the pipette was heat-polished, and its resistance was 3–5 megaohm. Series resistance was compensated by at least 70% in all recordings. The experiments were performed at room temperature (23–25 °C). Only one recording was performed on any one coverslip of cells to ensure that recordings were made from cells not previously exposed to chemical stimuli.

The extracellular control solution used for transiently transfected HaCaT and HEK293T cells contained: 160 mM NaCl, 2.5 mM KCl, 1 mM $CaCl_2$, 2 mM $MgCl_2$, 10 mM HEPES, 10 mM glucose, 320 mosmol, adjusted to pH 7.3 with NaOH. To obtain measurable current responses from endogenously expressed TRPV3 channels in HaCaT cells, $CaCl_2$ was replaced with 1 mM EGTA (Fig. 1). The pipette solution for HEK293T cells contained: 125 mM Cs-glucono-δ-lactone, 15 mM CsCl, 5 mM EGTA, 10 mM HEPES, 0.5 mM $CaCl_2$, 2 mM MgATP, 280 mosmol, adjusted to pH 7.3 with CsOH. The pipette solution for HaCaT cells contained: 125 mM Cs-glucono-δ-lactone, 15 mM CsCl, 5 mM EGTA, 10 mM HEPES, 0.5 mM $CaCl_2$, 1 mM $MgCl_2$, 2 mM MgATP, 0.3 mM NaGTP, 290 mosmol, adjusted to pH 7.3 with CsOH. Experimental solutions containing TRP channel agonists or signaling pathway modulators were always prepared fresh from stock solutions dissolved in DMSO. EGF was dissolved in 10 mM acetic acid at a concentration of 1 mg/ml and then diluted in 10% FBS in DMEM to its final concentration of 10 μg/ml. Bovine serum albumin in FBS served as a carrier of EGF and prevented the adsorption of this peptide onto the plastic material. A system for rapid superfusion of the cultured cells was used for drug application (30). All of the chemicals except for MEK1/2 inhibitor U0126 (Cell Signaling) were purchased from Sigma.

Data analysis

Electrophysiological data were analyzed in pCLAMP10 (Molecular Devices). Curve fitting and statistical analyses were done in SigmaPlot 10 (Systat Software). Statistical significance was determined using Student's *t* test or one-way analysis of variance followed by Dunnett's post hoc test, as appropriate. All data are presented as the mean ± S.D. unless stated otherwise.

Author contributions—L. V., S. B., and V. V. designed the study. L. V., S. B., L. M., and S. C. performed the experiments and analyzed the data. L. V. generated figures. L. V. and V. V. wrote and edited the paper.

Acknowledgments—We thank to Ardem Patapoutian (The Scripps Research Institute, San Diego, CA) for providing the human TRPV3 gene in pcDNA5/FRT vector, and Karel Harant and Pavel Talacko from the Laboratory of Mass Spectrometry, Biotechnology and Biomedicine, Center of the Academy of Sciences and Charles University in Vestec, where proteomic and mass spectrometric analysis had been done. Access to the MS facility was enabled by the European Union project CZ.1.05/1.1.00/02.0109. GFP-ERK1 was a gift from Rony Seger (Addgene plasmid number 14747).

References

1. Peier, A. M., Reeve, A. J., Andersson, D. A., Moqrich, A., Earley, T. J., Hergarden, A. C., Story, G. M., Colley, S., Hogenesch, J. B., McIntyre, P., Bevan, S., and Patapoutian, A. (2002) A heat-sensitive TRP channel expressed in keratinocytes. *Science* **296,** 2046–2049
2. Smith, G. D., Gunthorpe, M. J., Kelsell, R. E., Hayes, P. D., Reilly, P., Facer, P., Wright, J. E., Jerman, J. C., Walhin, J. P., Ooi, L., Egerton, J., Charles, K. J., Smart, D., Randall, A. D., Anand, P., and Davis, J. B. (2002) TRPV3 is a temperature-sensitive vanilloid receptor-like protein. *Nature* **418,** 186–190
3. Xu, H., Ramsey, I. S., Kotecha, S. A., Moran, M. M., Chong, J. A., Lawson, D., Ge, P., Lilly, J., Silos-Santiago, I., Xie, Y., DiStefano, P. S., Curtis, R., and Clapham, D. E. (2002) TRPV3 is a calcium-permeable temperature-sensitive cation channel. *Nature* **418,** 181–186

4. Nilius, B., and Biró, T. (2013) TRPV3: a "more than skinny" channel. *Exp. Dermatol.* **22,** 447–452
5. Nilius, B., Biró, T., and Owsianik, G. (2014) TRPV3: time to decipher a poorly understood family member! *J. Physiol.* **592,** 295–304
6. Luo, J., and Hu, H. (2014) Thermally activated TRPV3 channels. *Curr. Top. Membr.* **74,** 325–364
7. Yang, P., and Zhu, M. X. (2014) TRPV3 *Handb. Exp. Pharmacol.* **222,** 273–291
8. Bang, S., Yoo, S., Yang, T. J., Cho, H., and Hwang, S. W. (2010) Farnesyl pyrophosphate is a novel pain-producing molecule via specific activation of TRPV3. *J. Biol. Chem.* **285,** 19362–19371
9. Phelps, C. B., Wang, R. R., Choo, S. S., and Gaudet, R. (2010) Differential regulation of TRPV1, TRPV3, and TRPV4 sensitivity through a conserved binding site on the ankyrin repeat domain. *J. Biol. Chem.* **285,** 731–740
10. Xiao, R., Tang, J., Wang, C., Colton, C. K., Tian, J., and Zhu, M. X. (2008) Calcium plays a central role in the sensitization of TRPV3 channel to repetitive stimulations. *J. Biol. Chem.* **283,** 6162–6174
11. Hu, H. Z., Xiao, R., Wang, C., Gao, N., Colton, C. K., Wood, J. D., and Zhu, M. X. (2006) Potentiation of TRPV3 channel function by unsaturated fatty acids. *J. Cell. Physiol.* **208,** 201–212
12. Doerner, J. F., Hatt, H., and Ramsey, I. S. (2011) Voltage- and temperature-dependent activation of TRPV3 channels is potentiated by receptor-mediated PI(4,5)P2 hydrolysis. *J. Gen. Physiol.* **137,** 271–288
13. Liu, B., and Qin, F. (2017) Single-residue molecular switch for high-temperature dependence of vanilloid receptor TRPV3. *Proc. Natl. Acad. Sci. U.S.A.* **114,** 1589–1594
14. Liu, B., Yao, J., Zhu, M. X., and Qin, F. (2011) Hysteresis of gating underlines sensitization of TRPV3 channels. *J. Gen. Physiol.* **138,** 509–520
15. Billen, B., Brams, M., Debaveye, S., Remeeva, A., Alpizar, Y. A., Waelkens, E., Kreir, M., Brüggemann, A., Talavera, K., Nilius, B., Voets, T., and Ulens, C. (2015) Different ligands of the TRPV3 cation channel cause distinct conformational changes as revealed by intrinsic tryptophan fluorescence quenching. *J. Biol. Chem.* **290,** 12964–12974
16. Lin, Z., Chen, Q., Lee, M., Cao, X., Zhang, J., Ma, D., Chen, L., Hu, X., Wang, H., Wang, X., Zhang, P., Liu, X., Guan, L., Tang, Y., Yang, H., Tu, P., Bu, D., Zhu, X., Wang, K., Li, R., and Yang, Y. (2012) Exome sequencing reveals mutations in TRPV3 as a cause of Olmsted syndrome. *Am. J. Hum. Genet.* **90,** 558–564
17. Lai-Cheong, J. E., Sethuraman, G., Ramam, M., Stone, K., Simpson, M. A., and McGrath, J. A. (2012) Recurrent heterozygous missense mutation, p.Gly573Ser, in the *TRPV3* gene in an Indian boy with sporadic Olmsted syndrome. *Br. J. Dermatol.* **167,** 440–442
18. Moqrich, A., Hwang, S. W., Earley, T. J., Petrus, M. J., Murray, A. N., Spencer, K. S., Andahazy, M., Story, G. M., and Patapoutian, A. (2005) Impaired thermosensation in mice lacking TRPV3, a heat and camphor sensor in the skin. *Science* **307,** 1468–1472
19. Cheng, X., Jin, J., Hu, L., Shen, D., Dong, X. P., Samie, M. A., Knoff, J., Eisinger, B., Liu, M. L., Huang, S. M., Caterina, M. J., Dempsey, P., Michael, L. E., Dlugosz, A. A., Andrews, N. C., Clapham, D. E., and Xu, H. (2010) TRP channel regulates EGFR signaling in hair morphogenesis and skin barrier formation. *Cell* **141,** 331–343
20. Xu, H., Delling, M., Jun, J. C., and Clapham, D. E. (2006) Oregano, thyme and clove-derived flavors and skin sensitizers activate specific TRP channels. *Nat. Neurosci.* **9,** 628–635
21. Buscà, R., Pouysségur, J., and Lenormand, P. (2016) ERK1 and ERK2 MAP kinases: specific roles or functional redundancy? *Front. Cell. Dev. Biol.* **4,** 53
22. Stamboulian, S., Choi, J. S., Ahn, H. S., Chang, Y. W., Tyrrell, L., Black, J. A., Waxman, S. G., and Dib-Hajj, S. D. (2010) ERK1/2 mitogen-activated protein kinase phosphorylates sodium channel Na(v)1.7 and alters its gating properties. *J. Neurosci.* **30,** 1637–1647
23. Martin, S. W., Butcher, A. J., Berrow, N. S., Richards, M. W., Paddon, R. E., Turner, D. J., Dolphin, A. C., Sihra, T. S., and Fitzgerald, E. M. (2006) Phosphorylation sites on calcium channel α1 and β subunits regulate ERK-dependent modulation of neuronal N-type calcium channels. *Cell Calcium* **39,** 275–292
24. Shen, B., Kwan, H. Y., Ma, X., Wong, C. O., Du, J., Huang, Y., and Yao, X. (2011) cAMP activates TRPC6 channels via the phosphatidylinositol 3-kinase (PI3K)-protein kinase B (PKB)-mitogen-activated protein kinase kinase (MEK)-ERK1/2 signaling pathway. *J. Biol. Chem.* **286,** 19439–19445
25. Hu, H. J., Alter, B. J., Carrasquillo, Y., Qiu, C. S., and Gereau, R. W., 4th (2007) Metabotropic glutamate receptor 5 modulates nociceptive plasticity via extracellular signal-regulated kinase-Kv4.2 signaling in spinal cord dorsal horn neurons. *J. Neurosci.* **27,** 13181–13191
26. Shi, D. J., Ye, S., Cao, X., Zhang, R., and Wang, K. (2013) Crystal structure of the N-terminal ankyrin repeat domain of TRPV3 reveals unique conformation of finger 3 loop critical for channel function. *Protein Cell* **4,** 942–950
27. Karttunen, S., Duffield, M., Scrimgeour, N. R., Squires, L., Lim, W. L., Dallas, M. L., Scragg, J. L., Chicher, J., Dave, K. A., Whitelaw, M. L., Peers, C., Gorman, J. J., Gleadle, J. M., Rychkov, G. Y., and Peet, D. J. (2015) Oxygen-dependent hydroxylation by FIH regulates the TRPV3 ion channel. *J. Cell Sci.* **128,** 225–231
28. Hornbeck, P. V., Zhang, B., Murray, B., Kornhauser, J. M., Latham, V., and Skrzypek, E. (2015) PhosphoSitePlus, 2014: mutations, PTMs and recalibrations. *Nucleic Acids Res.* **43,** D512–520
29. Benedikt, J., Teisinger, J., Vyklicky, L., and Vlachova, V. (2007) Ethanol inhibits cold-menthol receptor TRPM8 by modulating its interaction with membrane phosphatidylinositol 4,5-bisphosphate. *J. Neurochem.* **100,** 211–224
30. Dittert, I., Benedikt, J., Vyklický, L., Zimmermann, K., Reeh, P. W., and Vlachová, V. (2006) Improved superfusion technique for rapid cooling or heating of cultured cells under patch-clamp conditions. *J. Neurosci. Methods* **151,** 178–185